Complexes of Importance to the Absorption of Solar Radiation†

ARTICLE *in* THE JOURNAL OF PHYSICAL CHEMISTRY A · OCTOBER 2003

Impact Factor: 2.69 · DOI: 10.1021/jp035098t

3 AUTHORS:

Henrik G Kjaergaard
University of Copenhagen
141 PUBLICATIONS **3,822** CITATIONS
SEE PROFILE

Timothy W. Robinson
ETH Zurich
18 PUBLICATIONS **430** CITATIONS
SEE PROFILE

Daryl L Howard
Australian Synchrotron
82 PUBLICATIONS **1,424** CITATIONS
SEE PROFILE

Complexes of Importance to the Absorption of Solar Radiation†

Henrik G. Kjaergaard,* Timothy W. Robinson, and Daryl L. Howard

Department of Chemistry, University of Otago, P.O. Box 56, Dunedin, New Zealand

John S. Daniel‡

NOAA Aeronomy Laboratory, Boulder, Colorado 80305

Jill E. Headrick and Veronica Vaida

Department of Chemistry and Biochemistry and CIRES, University of Colorado, Boulder, Colorado 80309

Received: April 24, 2003; In Final Form: August 27, 2003

Complexes of atmospheric molecules and atoms with water, $H_2O{\cdot}X$, where X is H_2O, N_2, O_2, Ar, and CO_2, are investigated to evaluate their possible role in the absorption of solar energy and consequently in influencing the Earth's climate. The atmospheric abundance and absorption spectra of these complexes are calculated and used in a line-by-line radiative transfer model to assess their contribution. We have used statistical mechanics to calculate equilibrium constants and the harmonically coupled anharmonic oscillator local mode model to calculate fundamental and overtone OH-stretching vibrational band frequencies and intensities. Parameters for these calculations were obtained with the use of ab initio methods. Apart from the water dimer, no OH-stretching bands are significantly frequency shifted compared to those in the water monomer, implying that observation of the vibrational spectra of these hydrates in the atmosphere will be difficult. Of the studied complexes, we find that the O_2 and N_2 monohydrates are likely to contribute the most to absorption of solar radiation; however, the absolute absorption is highly dependent on the band shape of the vibrational transitions.

Introduction

The Earth's temperature, climate, and chemistry are influenced by the absorption of solar radiation in the atmosphere. In this context, we discuss the role of weakly bound molecular complexes. Intermolecular interactions responsible for complexation alter the spectroscopy of the monomeric constituents.[1−5] The shifting and broadening of monomer spectral features, the appearance of new absorption bands, and the intensity enhancement of weak electronic transitions upon complexation could all have a significant atmospheric impact.[6−12]

The discrepancy between observed and modeled atmospheric absorption of solar radiation is a long-standing problem in atmospheric science.[13−15] Weakly bound van der Waals complexes, especially those containing water, have been suggested as possible contributors to the absorption of solar radiation[9,11,16−19] and might be associated[16] with the water vapor continuum.[20,21] The four most abundant species in a dry atmosphere are N_2, O_2, Ar, and CO_2. The next most abundant species, Ne, is about 20 times less abundant than CO_2.[22] Thus, we have considered the $H_2O{\cdot}X$ complexes, where X is H_2O, N_2, O_2, Ar, and CO_2. Atmospheric abundances and absorption spectra in the relevant spectral regions are needed to quantify the effect of these complexes on absorption of solar radiation. The atmospheric abundance of a complex scales with the partial pressures of the individual monomers and with its equilibrium constant.[11,12] The abundance of H_2O decreases rapidly with increasing altitude, due to both the pressure and temperature decrease, as illustrated in Figure 1.[22] The abundance of the water dimer, $H_2O{\cdot}H_2O$, depends on the square of the H_2O concentration and decreases more rapidly with altitude compared to the other $H_2O{\cdot}X$ complexes.[11,12]

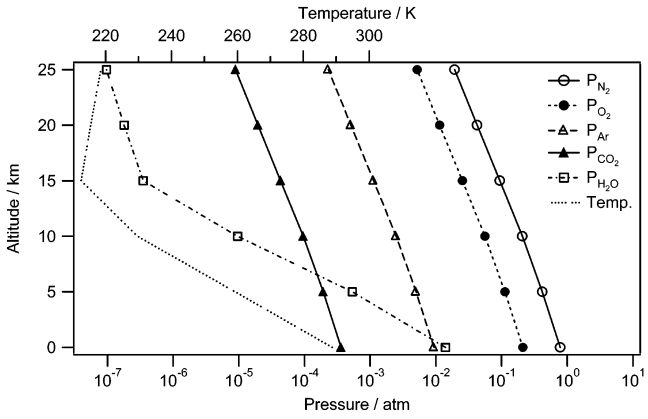

Figure 1. Atmospheric pressure of N_2, O_2, Ar, CO_2, and H_2O and the atmospheric temperature as a function of altitude.

Water vapor is a significant absorber of solar radiation in the near-infrared (NIR) and visible spectral regions. In these regions, absorption by H_2O is dominated by OH-stretching overtone transitions. These vibrations can be described in terms of local modes[23,24] and the harmonically coupled anharmonic oscillator (HCAO) local mode model.[25,26] Calculations on H_2O have shown that the simple HCAO local mode model provides intensities that are in good agreement with experiment.[27,28]

† Part of the special issue "Charles S. Parmenter Festschrift".

* To whom correspondence should be addressed. E-mail: henrik @alkali.otago.ac.nz. Fax: 64-3-479-7906. Phone: 64-3-479-5378.

‡ On sabbatical at Department of Chemistry, University of Otago, Dunedin, New Zealand.

10.1021/jp035098t CCC: $25.00
Published on Web 10/07/2003

Previous investigations of the vibrational spectra of $H_2O{\cdot}X$ have found that complexation causes only small perturbations to the fundamental frequencies of the monomer species for all complexes but the water dimer.[29−35] However, spectra of these weakly bound complexes are likely to have broadened band profiles compared with their monomeric constituents, which could therefore lead to additional atmospheric absorption of solar radiation outside the monomer absorption bands. Earlier field studies have failed to identify structured absorptions from $H_2O{\cdot}X$ complexes in the atmosphere.[36,37] However, very recently a single band observed in atmospheric near-infrared spectra was attributed to an OH-stretching overtone transition in water dimer.[38]

In this article, we report HCAO calculated fundamental and overtone OH-stretching band positions and intensities for the $H_2O{\cdot}X$ complexes and estimate the abundance of these complexes using equilibrium statistical thermodynamics. We have obtained all input parameters from ab initio calculations in order to provide a consistent comparison between the complexes investigated. Radiative transfer calculations are used to ascertain the relative impact of the $H_2O{\cdot}X$ complexes to atmospheric absorption of solar radiation.

Calculation of Absorption Spectra and Atmospheric Abundances

Recently, the HCAO local mode method has been used to calculate the OH-stretching vibrational band positions and intensities for the water dimer.[39] These calculations used dipole moment functions calculated with the quadratic configuration interaction including singles and doubles level of theory with a 6-311++G(2d,2p) basis set (QCISD/6-311++G(2d,2p)). The calculated OH-stretching transitions were in good agreement with those observed experimentally.[30,31,34,40] We have used the same ab initio method for the $H_2O{\cdot}X$ complexes investigated here. We refer to our previous papers for details on the calculation of fundamental and overtone OH-stretching transitions.[39,41]

We calculate the oscillator strength f of a transition from the ground vibrational state g to an excited vibrational state e from[26,42]

$$f_{eg} = 4.702 \times 10^{-7}[\text{cm D}^{-2}]\tilde{\nu}_{eg}|\vec{\mu}_{eg}|^2 \qquad (1)$$

where $\tilde{\nu}_{eg}$ is the wavenumber of the transition and $\vec{\mu}_{eg} = \langle e|\vec{\mu}|g\rangle$ is the transition dipole moment matrix element in Debye (D).

We use the HCAO local mode model to obtain the vibrational energies and wave functions required in eq 1. The water units of the $H_2O{\cdot}X$ complexes are either symmetric (two equivalent OH bonds) or asymmetric. The HCAO local mode equations for symmetric and asymmetric H_2O units are given elsewhere.[39,41] The local mode frequency $\tilde{\omega}$ and anharmonicity $\tilde{\omega}x$ for each of the OH bonds, and the parameter for the effective coupling between these γ, are obtained from ab initio calculations as detailed elsewhere.[39] The dipole moment function required in eq 1 is approximated by a series expansion in the internal OH displacement coordinates, with the expansion coefficients determined by ab initio calculations.[39,43]

The ab initio calculations were performed with the use of Gaussian 94.[44] Geometries were optimized with "tight" convergence limits and confirmed as minima by frequency calculations resulting in no imaginary frequencies. The electronic ground state of O_2 and $H_2O{\cdot}O_2$ is a triplet, and unrestricted wave functions have been used.

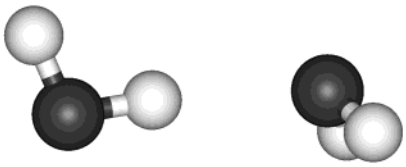

Figure 2. QCISD/6-311++G(2d,2p) optimized geometry of the $H_2O{\cdot}H_2O$ complex.

The temperature-dependent thermodynamic equilibrium constant $K(T)$ for the complexation reaction

$$H_2O(g) + X(g) \leftrightarrow H_2O{\cdot}X(g) \qquad (2)$$

is estimated using equilibrium statistical thermodynamics.[11,12,45] The partial pressure of the complex can be calculated from $K(T)$ by

$$P_{(H_2O\cdot X)} = K_p(T)P_{H_2O}P_X = K(T)P^o\left(\frac{P_{H_2O}}{P^o}\right)\left(\frac{P_X}{P^o}\right) = \frac{K(T)P_{H_2O}P_X}{P^o} \qquad (3)$$

where $K_p(T)$ is the equilibrium constant (in atm^{-1}), P_X and P_{H_2O} are the monomer partial pressures, and P^o is the standard reference pressure of 1 atm. The equilibrium constant can be determined from the standard enthalpy $\Delta H°$ and entropy $\Delta S°$ of the reaction by

$$K(T) = \exp\left(-\frac{\Delta G^o}{RT}\right) = \exp\left(\frac{-\Delta H^o + T\Delta S^o}{RT}\right) \qquad (4)$$

where ΔG^o is the standard Gibb's free energy change for the reaction. The details for calculation of ΔH^o and ΔS^o are given elsewhere.[12]

The accurate determination of the thermodynamic properties of complexes needed for the evaluation of the equilibrium constant is a difficult problem. At atmospheric temperatures (200−300 K), it is less likely that the equilibrium statistical mechanics model is adequate because of the resulting increase in intermolecular thermal motions within the molecular complex.[19,46] These motions can greatly perturb the structure, stability, and internal energy of the complex so that the equilibrium geometry is no longer an accurate description for the complex. This becomes a particular problem for the description of vibrational energy levels at and above the dissociation limit of the complexes. Recently, progress has been made toward a more complete statistical mechanics description for weakly bound complexes.[47−49] The abundance estimates for $H_2O{\cdot}X$ given here do not consider the problem of excited vibrational levels at and above dissociation and can only be taken as an approximate treatment of the thermodynamics of weakly bound complexes.

The vibrational frequencies, rotational constants, rotational symmetry numbers, electronic energies, and degeneracy of the electronic states of both monomers and complexes are required in the statistical thermodynamics calculation. These parameters were obtained from QCISD/6-311++G(2d,2p) ab initio calculations and are given as supporting information Table 1S.

Results and Discussion

Structures of the Complexes. The QCISD/6-311++G(2d,2p) optimized structures for the five complexes $H_2O{\cdot}X$ are shown in Figures 2−6. The structures of the complexes,

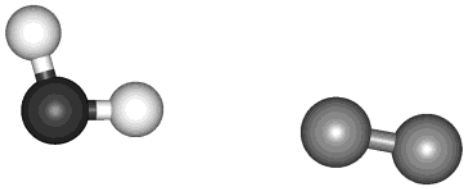

Figure 3. QCISD/6-311++G(2d,2p) optimized geometry of the $H_2O\cdot N_2$ complex.

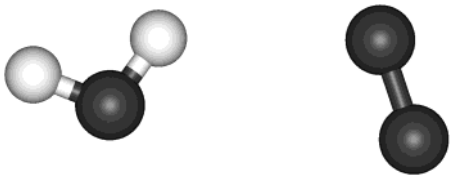

Figure 4. QCISD/6-311++G(2d,2p) optimized geometry of the $H_2O\cdot O_2$ complex.

Figure 5. QCISD/6-311++G(2d,2p) optimized geometry of the $H_2O\cdot$ Ar complex.

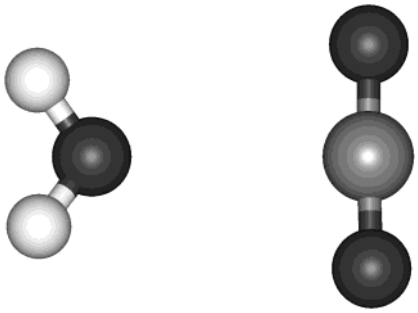

Figure 6. QCISD/6-311++G(2d,2p) optimized geometry of the $H_2O\cdot CO_2$ complex.

TABLE 1: Calculated and Observed Binding Energy, Permanent Dipole Moment, and O···X Distance

	E_b (kcal/mol)		$\vec{\mu}$ (D)		$R_{O\cdots X}$ (Å)[b]	
	calc.[a]	expt.	calc.[a]	expt.	calc.[a]	expt.
H_2O			1.96	1.850[e]		
$H_2O\cdot$Ar	0.32	0.41[c]	1.98		3.895	3.636[c]
$H_2O\cdot O_2$	0.72		1.80		3.226	–
$H_2O\cdot N_2$	1.29		2.08		3.350	3.37[h]
$H_2O\cdot CO_2$	2.73		2.24	1.852[f]	2.816	2.836[f]
$H_2O\cdot H_2O$	5.09	4.91[d]	2.68	2.643[g]	2.942	2.98[g]

[a] Calculated with the QCISD/6-311++G(2d,2p) method. [b] Distance from the O atom of the water unit to the nearest heavy atom. [c] Cohen and Saykally.[52] [d] Goldman et al.[47] [e] Dyke and Muenter.[62] [f] Peterson and Klemperer.[51] [g] Dyke et al.[63] [h] Leung et al.[53]

except $H_2O\cdot O_2$ have also been determined experimentally.[50−53] All structures have C_s symmetry. The structures of the $H_2O\cdot X$ complexes, except $X = CO_2$, have an H atom of the H_2O unit involved in an O−H···X bond. In Table 1, we compare the calculated and experimental binding energy, permanent dipole moment, and the equilibrium distance from the O atom of the H_2O unit to the nearest heavy atom ($R_{O\cdots X}$) for each of the complexes. The largest discrepancy in geometry is for the $H_2O\cdot$Ar complex, where the calculated $R_{O\cdots X}$ distance is 0.2 Å longer than the experimental value. For the other complexes, the agreement is good, and for this reason, we have used the QCISD/6-311++G(2d,2p) calculated rotational constants in the abundance calculations. For H_2O and $H_2O\cdot H_2O$, the QCISD/6-311++G(2d,2p) calculated dipole moments of the optimized structures agree well with the experimental values, whereas for $H_2O\cdot CO_2$, there is some discrepancy.

TABLE 2: Local Mode Parameters (cm^{-1})[a]

	OH_b		OH		
	$\tilde{\omega}$	$\tilde{\omega}x$	$\tilde{\omega}$	$\tilde{\omega}x$	γ
H_2O[b,c]			3869.9	82.06	49.44
$H_2O\cdot$Ar	3869	82.1	3871	81.8	47.1
$H_2O\cdot O_2$	3869	82.1	3870	81.8	48.3
$H_2O\cdot N_2$	3872	82.2	3873	81.0	47.2
$H_2O\cdot CO_2$[b]			3869	81.9	48.1
$H_2O\cdot H_2O$[d]	3781	85.4	3878	82.2	43.8
$H_2O\cdot H_2O$[b,e]			3863	81.7	46.1

[a] Calculated with the QCISD/6-311++G(2d,2p) method and scaled with 0.9836 and 0.851 for $\tilde{\omega}$ and $\tilde{\omega}x$, respectively. [b] The two OH bonds in these water units are equivalent. [c] Experimental local mode parameters for the water monomer.[27] [d] The hydrogen donor unit of the water dimer. [e] The hydrogen acceptor unit of the water dimer.

The water dimer has the largest binding energy of the complexes studied. The calculated binding energy of 5.1 kcal/mol is in good agreement with the measured binding energies of 4.9[47] and 5.4 kcal/mol.[54] The calculated binding energy of $H_2O\cdot$Ar is 0.32 kcal/mol, which compares well with an experimental value of 0.41 kcal/mol.[52] Based on these results, we estimate the uncertainty in the calculated binding energies to be about ±0.2 kcal/mol.

Vibrational Spectra. The OH-stretching fundamental and overtone frequencies and intensities were calculated with our HCAO local mode model.[39,41] We have also calculated the infrared vibrational frequencies and intensities of the $H_2O\cdot X$ complexes with a harmonic oscillator (normal mode) linear dipole moment (HOLD) approximation.

The local mode parameters are obtained from QCISD/6-311++G(2d,2p) calculated OH-stretching potential energy curves[39] and are given in Table 2. To compensate for inaccuracy in the ab initio method, the parameters are multiplied by scaling factors determined as the ratio of experimental to calculated $\tilde{\omega}$ (and $\tilde{\omega}x$) for H_2O.[39] The scaling factors are given in the footnote to Table 2. Apart from the OH oscillator involved in the hydrogen bonding (OH_b) of the water dimer, no significant change is observed for the local mode frequency and anharmonicity compared to the water monomer.

In Figure 7, we show the simulated OH-stretching vibrational spectra of the $H_2O\cdot X$ complexes in the $\Delta v_{OH} = 4$ region (4 quanta in the OH-stretching vibrations). Each OH-stretching transition has been convolved with a Lorentzian line profile with a full width at half-maximum (fwhm) of 40 cm^{-1}. For comparison, we show a simulated water monomer spectrum, generated from the experimental transitions convolved with Gaussian line profiles with fwhm of 2 cm^{-1}.[28] The H_2O spectrum contains rotational P and R branches of two bands: the strong $|40\rangle_{\pm}$ band and the weaker higher energy $|31\rangle_{-}$ band. We use the local mode notation, in which $|40\rangle_{\pm}$ represents the pure local mode states with all the vibrational energy in one of the OH bonds. The local mode combination states $|31\rangle_{+}$ and $|31\rangle_{-}$ have energy in both the OH bonds. The ± indicates the symmetry of the state. The OH-stretching bands of the complexes except the water dimer are not significantly shifted from the center of H_2O bands, and the relative intensities of the two bands are similar to that observed for H_2O. The much

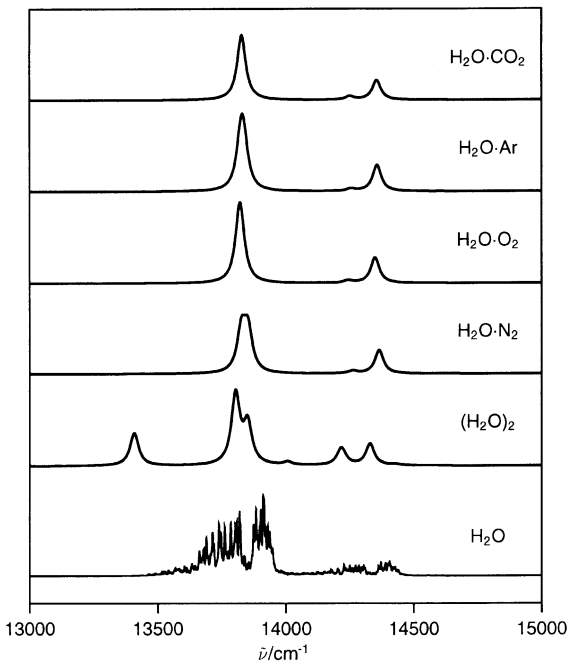

Figure 7. Simulated spectra of $H_2O{\cdot}N_2$, $H_2O{\cdot}O_2$, $H_2O{\cdot}Ar$, $H_2O{\cdot}CO_2$, and $H_2O{\cdot}H_2O$ in the $\Delta\upsilon_{OH} = 4$ region. The OH-stretching vibrational transitions were calculated with the QCISD/6-311++G(2d,2p) method and convolved with Lorentzian functions with a fwhm of 40 cm^{-1}. The experimental water spectrum was taken from the HITRAN database and was convolved with Gaussian functions with a fwhm of 2 cm^{-1} for illustrative purposes.

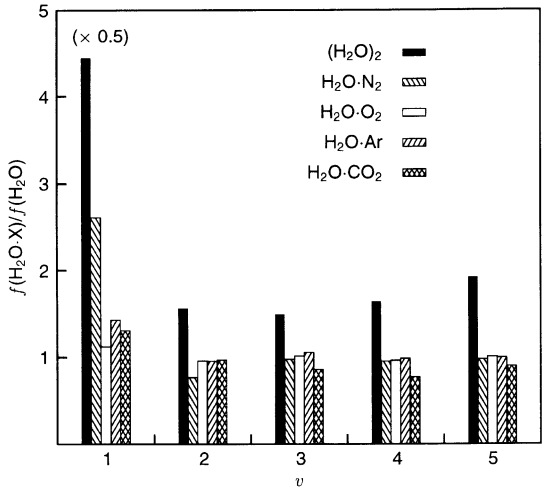

Figure 8. Ratio of calculated total OH-stretching oscillator strengths of $H_2O{\cdot}H_2O$, $H_2O{\cdot}N_2$, $H_2O{\cdot}O_2$, $H_2O{\cdot}Ar$, and $H_2O{\cdot}CO_2$ to that of H_2O as a function of $\Delta\upsilon_{OH}$. All calculated with the QCISD/6-311++G(2d,2p) method.

weaker $|31\rangle_+$ band is barely noticeable between the two stronger bands. The rotational structure in the experimental H_2O spectrum is not expected to be present in the spectra of the complexes, because of their shorter lifetimes.

Both fundamental and overtone transitions are important in the total atmospheric absorption of solar radiation. In Figure 8, we show the ratio of total OH-stretching intensity of the complexes to that of H_2O. In the fundamental region, $H_2O{\cdot}H_2O$ and $H_2O{\cdot}N_2$, and to a much lesser extent $H_2O{\cdot}Ar$, $H_2O{\cdot}CO_2$, and $H_2O{\cdot}O_2$, show increased OH-stretching intensity relative to that of H_2O. In the overtone regions, the ratio is close to unity for all complexes except the water dimer, for which the total intensity approaches roughly twice that of H_2O as υ_{OH} increases.[39] For the first overtone, there is a significant drop in the intensity of the hydrogen bonded OH_b-stretching transition in water dimer.[34,39,41]

Significant frequency shifts and intensity changes have been found for some of the fundamental vibrations of the water dimer compared to the water monomer,[31,34,35,38−40] whereas only minor changes have been found for the other complexes.[29,33,41,55,56] For the water dimer, the HCAO calculated OH-stretching vibrations are within 10 cm^{-1} of the transitions observed in molecular beam experiments. The HCAO calculated fundamental frequencies of the OH-stretching transitions of all complexes agree well with existing matrix isolation observations if matrix frequency red shifts are considered. For $H_2O{\cdot}H_2O$ and $H_2O{\cdot}N_2$, the HCAO calculated OH-stretching transitions are about 25 cm^{-1} higher in energy than those observed in the Ar matrix.[33,34,57] The asymmetric υ_3 ($|10\rangle_-$) vibration of $H_2O{\cdot}Ar$ is somewhat surprisingly observed[32] at 3782 cm^{-1}, which is 20 cm^{-1} higher than the υ_3 vibration in H_2O and 28 cm^{-1} higher than the HCAO calculated asymmetric OH-stretching transition in the complex. The HOLD calculated harmonic frequencies are higher than the observed fundamental transitions as expected with a QCISD/6-311++G(2d,2p) calculation. The OH-stretching harmonic frequencies are about 200 cm^{-1} higher than the observed fundamental transitions, which is close to the difference expected from the neglect of anharmonicity. These harmonic frequencies have been used in the statistical thermodynamics calculation.

All HCAO calculated OH-stretching transitions in H_2O and $H_2O{\cdot}X$ are given in the Supporting Information in Tables 2S−7S, and the HOLD calculated fundamental frequencies and intensities are given in Table 8S.

Atmospheric Abundances. We have used an equilibrium statistical thermodynamics procedure and a simple atmospheric model to calculate the equilibrium constants and atmospheric partial pressures of the $H_2O{\cdot}X$ complexes for altitudes up to 50 km.[12] Calculated values of $K_p(T)$ for each of the complexes at different altitudes are given in the Supporting Information in Table 9S for a standard atmosphere.[22] The variation with altitude of the calculated $K_p(T)$ ranges from negligible for $H_2O{\cdot}O_2$ and $H_2O{\cdot}Ar$, to a factor of 10 for $H_2O{\cdot}H_2O$. For all complexes, apart from $H_2O{\cdot}O_2$, $K_p(T)$ increases with decreasing temperature.

In Figure 9, we show the calculated variation in partial pressure of the complexes with altitude, obtained using the partial pressure of the monomeric species and the atmospheric temperature given in Figure 1.[22] The general increase in $K_p(T)$ toward the tropopause does not compensate for the rapid decrease in concentration of all monomeric species with increasing altitude. Thus, the abundance of all complexes is largest at ground level and decreases with increasing altitude. The partial pressure of $H_2O{\cdot}H_2O$ decreases more rapidly with altitude because of its dependence on the square of the partial pressure of H_2O. The $H_2O{\cdot}H_2O$ complex has a larger $K_p(T)$ than $H_2O{\cdot}N_2$ and $H_2O{\cdot}O_2$; however, its abundance is lower due to the significantly lower partial pressure of H_2O compared to N_2 and O_2. The $H_2O{\cdot}N_2$ and $H_2O{\cdot}O_2$ complexes are the most abundant and are roughly a factor of 5 more abundant than $H_2O{\cdot}H_2O$ and $H_2O{\cdot}Ar$ at ground level and about 2 orders of magnitude more abundant than $H_2O{\cdot}CO_2$. Previously, the abundances of $H_2O{\cdot}N_2$ and $H_2O{\cdot}O_2$ have been estimated to be an order of magnitude larger than that of the water dimer,[9,12,56] in reasonable agreement with the present calculation at ground level. The rapid decrease in abundance with altitude indicates that the $H_2O{\cdot}X$ complexes are unlikely to have any impact on the absorption of solar radiation above the tropopause.

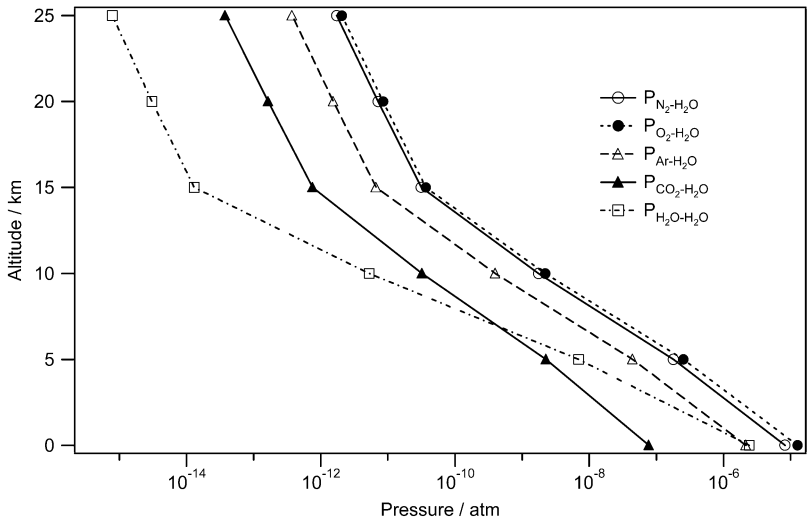

Figure 9. Calculated atmospheric pressures of $H_2O{\cdot}N_2$, $H_2O{\cdot}O_2$, $H_2O{\cdot}Ar$, $H_2O{\cdot}CO_2$, and $H_2O{\cdot}H_2O$ as a function of altitude.

We have estimated the sensitivity of our calculated abundances to the ab initio calculated input parameters. We estimate the uncertainty in calculated binding energies to be ±0.2 kcal/mol, and we have tested the effect on $K_p(T)$ of this uncertainty. We also tested the effect of a ±10% change in the harmonic frequencies on $K_p(T)$. The ±0.2 kcal/mol change in binding energy leads to changes in $K_p(T)$ of less than about 50% for all complexes over the entire altitude range. The ±10% change in frequencies leads to a maximal change of about a factor of 2 in $K_p(T)$.

Thermal conductivity measurements for $H_2O{\cdot}H_2O$ at 373 K lead to an experimentally determined K_p of 0.011 atm^{-1}.[54] Our calculated value at that temperature is 0.0034 atm^{-1}, whereas that calculated by Kim et al.[58] is 0.0025 atm^{-1}. Kim et al.[58] determined a free-energy lowering for $H_2O{\cdot}H_2O$ of 0.53 kcal/mol due to hindered internal rotation, which increases their K_p to 0.0066 atm^{-1}, closer to the experimental value. At 296 K, we obtain a K_p value of 0.011 atm^{-1}, with the estimated uncertainty giving a range from 0.006 atm^{-1} to 0.026 atm^{-1}, compared to a recently calculated value of 0.1 atm^{-1}.[47] Considering the previous comparisons, we suggest that our calculated abundances are reasonable estimates to within an order of magnitude.

As mentioned, the equilibrium statistical thermodynamics approach may be less appropriate as the energy of the complexes approaches the dissociation energy, which for all these complexes occurs even at IR energies. As Goldman et al.[47] point out, as the highly nonrigid water dimer accesses higher excited rotational states, the values of the rotational constants will decrease, causing a corresponding increase in $K_p(T)$. Failure to account for this effect will result in underestimating the value of $K_p(T)$. This may be one reason our calculated $K_p(T)$ values for water dimer are lower than the experimentally determined equilibrium constants.[54]

Radiative Transfer Simulations and Solar Absorption. An estimate of the atmospheric solar absorption of the $H_2O{\cdot}X$ complexes cannot accurately be made simply from the absorption cross sections and abundances. Because of the strong absorption of the water monomer in the NIR, it is important to consider the amount of spectral overlap between the strong, structured H_2O rovibrational absorption lines and the weaker vibrational absorption bands of the complexes. We have used a line-by-line multiple scattering model to estimate the relative importance of the various complexes to atmospheric absorption of solar radiation. Details of the radiative transfer model used are described elsewhere.[11,37]

TABLE 3: Total Absorption of Solar Radiation (Wm^{-2}) for a Tropical Case with Overhead Sun as a Function of the Assigned Band Width and Shape

	Lorentzian			Gaussian		truncated Lorentzian	
	20[a]	40[a]	250[a]	20[a]	250[a]	20[a,b]	20[a,c]
$H_2O{\cdot}Ar$	0.11	0.21	1.15	0.016	0.043	0.080	0.016
$H_2O{\cdot}O_2$	0.56	1.02	5.42	0.086	0.23	0.40	0.085
$H_2O{\cdot}N_2$	0.68	1.29	6.91	0.066	0.20	0.47	0.064
$H_2O{\cdot}CO_2$	0.004	0.007	0.040	0.0005	0.0014	0.003	0.0005
$H_2O{\cdot}H_2O$	0.44	0.85	4.76	0.019	0.14	0.28	0.019

[a] fwhm in cm^{-1}. [b] Far wings cut off at ±1000 cm^{-1}. [c] Far wings cut off at ±100 cm^{-1}.

In this study, the atmosphere is divided into 35 homogeneous layers, with the lowest 20 layers 1 km thick, and the top 15 layers 2 km thick. The surface temperature is assumed to be 298 K, and the lapse rate is 4.5 K/km for the lowest 18 km. Monomers included in the atmosphere are H_2O, O_2, and CO_2. The H_2O vertical profile is calculated assuming a constant tropospheric relative humidity of 57%, yielding a column abundance of 45 mm precipitable water (1.5×10^{23} molecules/cm^2), consistent with the July tropical average.[59] The CO_2 mixing ratio is taken to be 370 ppm. Absorption coefficients for the monomers are calculated considering both pressure and temperature broadening using the HITRAN 2000 line list with the updated water vapor list.[28] For the $H_2O{\cdot}X$ complexes, we use our equilibrium constants at the relevant temperatures to estimate the abundances from the monomer concentrations. The absorption spectra are obtained by convolving our calculated OH-stretching transitions with a given line shape and width. The absorption coefficients of each monomer considered are calculated every 0.01 cm^{-1} and each complex every 0.1 cm^{-1} from 2000 cm^{-1} (5.0 μm) to 25 000 cm^{-1} (400 nm).[37] The multiple scattering calculations are performed every 0.01 cm^{-1} over the same wavelength range using a discrete ordinates formalism and considering 4 intensity streams. In these simulations of the tropical atmosphere, we assumed an overhead sun, no aerosols and a surface albedo of 0.15.

The total integrated absorption of sunlight for each of the complexes is given in Table 3 and is obtained by differencing the calculated total absorption with and without the complex. The total absorption by $H_2O{\cdot}H_2O$ has previously been found to

be sensitive to the assigned bandwidth of the absorption bands.[11] The actual bandwidth would depend on both the rotational constants and the lifetime of the complex. Without dynamical information, the line widths cannot accurately be obtained. As an example, the observed electronic transitions in the $O_2 \cdot O_2$ collision induced complex are broad bands with fwhm of approximately 350 cm^{-1}, without the rotationally resolved structure observed in O_2 spectra.[60] The fundamental OH-stretching transitions of the $H_2O \cdot H_2O$ complex have been observed to have a fwhm of about 15 cm^{-1} and the third overtone OH_b-stretching band in water dimer a fwhm of about 19 cm^{-1}.[38] So although we expect unstructured bands in the $H_2O \cdot X$ complexes, the large uncertainty in the details of the band shape leads us to consider several bandwidths and shapes. We have tested Lorentzian band shapes with fwhm of 20, 40, and 250 cm^{-1}, Gaussian band shapes with fwhm of 20 and 250 cm^{-1}, and truncated Lorentzian band shapes with a fwhm of 20 cm^{-1}, for which we have cut the absorption to zero in the wings at either ± 1000 cm^{-1} or ± 100 cm^{-1} from the band center and renormalized the band intensities so there is no loss of integrated absorption strength.

For all of the band shapes and widths considered in Table 3, it is clear that $H_2O \cdot O_2$ and $H_2O \cdot N_2$ absorb the most, whereas there is negligible absorption from $H_2O \cdot CO_2$, due primarily to the small concentration of CO_2 in the atmosphere. If the 20 cm^{-1} Lorentzian case is considered, for example, the amount of absorption by $H_2O \cdot H_2O$ (0.44 W/m^2) is only about a third of the total absorption by the other complexes (1.35 W/m^2). The calculated total absorption by $H_2O \cdot H_2O$ in the 40 cm^{-1} Lorentzian case is smaller than our previously published value, partly because the HOH-bending transitions have not been included in the present calculations, but also because a column water vapor amount of 65 mm rather than the stated 45 mm was inadvertently used in the previously calculated tropical scenario.[11] The water dimer equilibrium constants used in the present calculations are between the low and high estimates of the previous study.[11]

One of the most important points illustrated by Table 3 is the significant effect of the band shape on the total complex absorption. As the intensity is spread further away from the band center to the wings, the absorption increases because the overlap with water monomer absorption becomes less. The Gaussian band shape simulations have substantially less total atmospheric absorption because of the inherently smaller wings compared to the Lorentzian band shape.

To further illustrate the importance of the far wings, the final two columns of Table 3 show the total absorption for the 20 cm^{-1} Lorentzian band shape with wing cutoffs at ± 1000 cm^{-1} and ± 100 cm^{-1}, respectively. For each complex, it is apparent that cutting off the wings at ± 1000 cm^{-1} reduces the total absorption by less than 40%. In contrast, the ± 100 cm^{-1} cutoff reduces the absorption by 85−95%. Accurate knowledge of the band shapes of the complexes far from the band center is likely to be very difficult to obtain experimentally, just as it is for the water vapor monomer line shape.[61]

Because of the large variation of water vapor in the atmosphere, it is also important to understand how the values in Table 3 change for various atmospheric water vapor amounts. Absorption calculations have been made for a water vapor column half as large as that assumed for the estimates summarized in Table 3 by reducing the relative humidity by a factor of 2 at all altitudes. In the absence of the spectral overlap with the water monomer absorption, the absorption by the water dimer would be reduced by a factor of 4 and for the other clusters by a factor of 2. With monomer overlap considered, the dimer absorption is reduced by a factor of 3.3 and the other clusters by approximately a factor of 1.7. Thus, the relative impact of the complexes increases as the amount of water in the atmosphere decreases.

Conclusion

We have calculated the frequencies and intensities of the OH-stretching transitions up to 25 000 cm^{-1} for $H_2O \cdot X$ complexes where X is H_2O, N_2, O_2, Ar, and CO_2. Of the complexes investigated, only $H_2O \cdot H_2O$ has significantly frequency-shifted OH-stretching transitions due to hydrogen bonding, making it the most likely candidate for identification in the atmosphere.

We have used the calculated OH-stretching frequencies and intensities and the estimated atmospheric abundances of these complexes in line-by-line radiative transfer simulations of the propagation of solar radiation through the atmosphere. Our simulations indicate that of the complexes considered, $H_2O \cdot O_2$ and $H_2O \cdot N_2$ are the largest absorbers, with $H_2O \cdot Ar$ and $H_2O \cdot H_2O$ providing nonnegligible absorption. The calculated total absorption for each of the complexes is highly dependent on the assumed band shape and width. In particular, we note the importance of the band shape far from band center.

Acknowledgment. We would like to thank Daniel P. Schofield for helpful discussions. J.S.D. would like to thank University of Otago for kind hospitality during a visit. H.G.K. is grateful to CIRES for a visiting faculty fellowship. The Marsden Fund administrated by the Royal Society of New Zealand, the University of Otago, and the National Science Foundation have provided funding for this research.

Supporting Information Available: One table with input parameters for $K(T)$ calculation. Six tables with calculated OH-stretching transitions in H_2O and the $H_2O \cdot X$ complexes. One table with calculated harmonic frequencies and intensities of the monomers and complexes. One table with calculated K values at different altitudes. This material is available free of charge via the Internet at http://pubs.acs.org.

References and Notes

(1) Miller, R. E. *Acc. Chem. Res.* **1990**, *23*, 10.
(2) Bernstein, E. R. *Annu. Rev. Phys. Chem.* **1995**, *46*, 197.
(3) Leopold, K. R.; Canagaratna, M.; Phillips, J. A. *Acc. Chem. Res.* **1997**, *30*, 57.
(4) Aloisio, S.; Francisco, J. S. *Acc. Chem. Res.* **2000**, *33*, 825.
(5) Vaida, V.; Kjaergaard, H. G.; Feierabend, K. J. *Int. Rev. Phys. Chem.* **2003**, *22*, 203.
(6) Molina, L. T.; Molina, M. J. *J. Phys. Chem.* **1987**, *91*, 433.
(7) Kolb, C. E.; Jayne, J. T.; Worsnop, D. R.; Molina, M. J.; Meads, R. F.; Viggiano, A. A. *J. Am. Chem. Soc.* **1994**, *116*, 10314.
(8) Frost, G. J.; Vaida, V. *J. Geophys. Res.* **1995**, *100*, 18803.
(9) Chylek, P.; Geldart, D. J. W. *Geophys. Res. Lett.* **1997**, *24*, 2015.
(10) Pfeilsticker, K.; Erle, F.; Platt, U. *J. Atmos. Sci.* **1997**, *54*, 933.
(11) Vaida, V.; Daniel, J. S.; Kjaergaard, H. G.; Goss, L. M.; Tuck, A. F. *Q. J. R. Meteor. Soc.* **2001**, *127*, 1627.
(12) Vaida, V.; Headrick, J. E. *J. Phys. Chem. A* **2000**, *104*, 5401.
(13) Li, Z.; Barker, H. W.; Moreau, L. *Nature* **1995**, *376*, 486.
(14) Ramanathan, V.; Subasilar, B.; Zhang, G. J.; Conant, W.; Cess, R. D.; Kiehl, J. T.; Grassl, H.; Shi, L. *Science* **1995**, *267*, 499.
(15) Pilewskie, P.; Valero, F. P. J. *Science* **1995**, *267*, 1626.
(16) Varanasi, P.; Chou, S.; Penner, S. S. *J. Quant. Spectrosc. Radiat. Transfer* **1968**, *8*, 1537.
(17) Bignell, K. J. *Q. J. R. Meteor. Soc.* **1970**, *96*, 390.
(18) Carlon, H. R. *Infrared Phys.* **1979**, *19*, 549.
(19) Vigasin, A. A. Molecular Complexes in Earth's Planetary, Cometary and Interstellar Atmospheres. In *Molecular Complexes in Earth's Planetary, Cometary and Interstellar Atmospheres.*; Vigasin, A. A., Slanina, Z., Eds.; World Scientific: River Edge, NJ, 1998.

(20) Clough, S. A.; Kneizys, F. X.; Davies, R.; Gamache, R.; Tipping, R. In *Atmospheric Water Vapor*; Deepak, A., Wilkerson, T. D., Ruhnke, L. H., Eds.; Academic Press: New York, 1980.
(21) Clough, S. A.; Kneizys, F. X.; Davies, R. W. *Atmos. Res.* **1989**, *23*, 229.
(22) Brasseur, G. P.; Solomon, S. *Aeronomy of the middle atmosphere*; D. Reidel Publishing Co.: Dordrecht, Holland, 1984.
(23) Henry, B. R. *Acc. Chem. Res.* **1977**, *10*, 207.
(24) Henry, B. R.; Kjaergaard, H. G. *Can. J. Chem.* **2002**, *80*, 1635.
(25) Mortensen, O. S.; Henry, B. R.; Mohammadi, M. A. *J. Chem. Phys.* **1981**, *75*, 4800.
(26) Kjaergaard, H. G.; Yu, H.; Schattka, B. J.; Henry, B. R.; Tarr, A. W. *J. Chem. Phys.* **1990**, *93*, 6239.
(27) Kjaergaard, H. G.; Henry, B. R.; Wei, H.; Lefebvre, S.; Carrington, T., Jr.; Mortensen, O. S.; Sage, M. L. *J. Chem. Phys.* **1994**, *100*, 6228.
(28) Rothman, L. S.; Rinsland, C. P.; Goldman, A.; Massie, S. T.; Edwards, D. P.; Flaud, J.-M.; Perrin, A.; Camy-Peyret, C.; Dana, V.; Mandin, J.-Y.; Schroeder, J.; McCann, A.; Gamache, R. R.; Wattson, R. B.; Yoshino, K.; Chance, K. V.; Jucks, K. W.; Brown, L. R.; Nemtchinov, V.; Varanasi, P. *J. Quant. Spectrosc. Radiat. Transfer* **1998**, *60*, 665.
(29) Tso, T.-L.; Lee, K. C. *J. Phys. Chem.* **1985**, *89*, 1612.
(30) Huang, Z. S.; Miller, R. E. *J. Chem. Phys.* **1989**, *91*, 6613.
(31) Huisken, F.; Kaloudis, M.; Kulcke, A. *J. Chem. Phys.* **1996**, *104*, 17.
(32) Nesbitt, D. J.; Lascola, R. *J. Chem. Phys.* **1992**, *97*, 8096.
(33) Coussan, S.; Loutellier, A.; Perchard, J. P.; Racine, S.; Bouteiller, Y. *J. Mol. Struct.* **1998**, *471*, 37.
(34) Perchard, J. P. *Chem. Phys.* **2001**, *273*, 217.
(35) Liu, K.; Cruzan, J. D.; Saykally, R. J. *Science* **1996**, *271*, 929.
(36) Hill, C.; Jones, R. L. *J. Geophys. Res.* **2000**, *105*, 9421.
(37) Daniel, J. S.; Solomon, S.; Sanders, R. W.; Portmann, R. W.; Miller, D. C.; Madsen, W. *J. Geophys. Res., D: Atmos.* **1999**, *104*, 16785.
(38) Pfeilsticker, K.; Lotter, A.; Peters, C.; Bosch, H. *Science* **2003**, *300*, 2078.
(39) Low, G. R.; Kjaergaard, H. G. *J. Chem. Phys.* **1999**, *110*, 9104.
(40) Perchard, J. P. *Chem. Phys.* **2001**, *266*, 109.
(41) Kjaergaard, H. G.; Low, G. R.; Robinson, T. W.; Howard, D. L. *J. Phys. Chem. A* **2002**, *106*, 8955.
(42) Atkins, P. W.; Friedman, R. S. *Molecular Quantum Mechanics*, 3rd ed.; Oxford University Press: Oxford, 1997.
(43) Kjaergaard, H. G.; Henry, B. R. *J. Chem. Phys.* **1992**, *96*, 4841.
(44) Frisch, M. J.; Trucks, G. W.; Schlegel, H. B.; Gill, P. M. W.; Johnson, B. G.; Robb, M. A.; Cheeseman, J. R.; Keith, T.; Petersson, G. A.; Montgomery, J. A.; Raghavachari, K.; Al-Laham, M. A.; Zakrzewski, V. G.; Ortiz, J. V.; Foresman, J. B.; Cioslowski, J.; Stefanov, B. B.; Nanayakkara, A.; Challacombe, M.; Peng, C. Y.; Ayala, P. Y.; Chen, W.; Wong, M. W.; Andres, J. L.; Replogle, E. S.; Gomperts, R.; Martin, R. L.; Fox, D. J.; Binkley, J. S.; Defrees, D. J.; Baker, J.; Stewart, J. P.; Head-Gordon, M.; Gonzalez, C.; Pople, J. A. *Gaussian 94*, revision D.4; Gaussian, Inc.: Pittsburgh, PA, 1995.
(45) McQuarrie, D. A. *Statistical Mechanics*; Harper Collins: New York, 1976.
(46) Schenter, G. K. *J. Chem. Phys.* **1998**, *108*, 6222.
(47) Goldman, N.; Fellers, R. S.; Leforestier, C.; Saykally, R. J. *J. Phys. Chem. A* **2001**, *105*, 515.
(48) Fellers, R. S.; Braly, L. B.; Saykally, R. J.; Leforestier, C. *J. Chem. Phys.* **1999**, *110*, 6306.
(49) Schenter, G. K.; Kathmann, S. M.; Garrett, B. C. *J. Phys. Chem. A* **2002**, *106*, 1557.
(50) Dyke, T. R. *J. Chem. Phys.* **1977**, *66*, 492.
(51) Peterson, K. I.; Klemperer, W. *J. Chem. Phys.* **1984**, *80*, 2439.
(52) Cohen, R. C.; Saykally, R. J. *J. Chem. Phys.* **1993**, *98*, 6007.
(53) Leung, H. O.; Marshall, M. D.; Suenram, R. D.; Lovas, F. J. *J. Chem. Phys.* **1989**, *90*, 700.
(54) Curtiss, L. A.; Frurip, D. J.; Blander, M. *J. Chem. Phys.* **1979**, *71*, 2703.
(55) Andrews, L.; Davis, S. R. *J. Chem. Phys.* **1985**, *83*, 4983.
(56) Svishchev, I. M.; Boyd, R. J. *J. Phys. Chem. A* **1998**, *102*, 7294.
(57) Schofield, D. P.; Kjaergaard, H. G. *Phys. Chem. Chem. Phys.* **2003**, *5*, 3100.
(58) Kim, K. S.; Mhin, B. J.; Choi, U. S.; Lee, K. *J. Chem. Phys.* **1992**, *97*, 6649.
(59) Randal, D. L.; Greenwald, T. H.; Vonder Haar, T. H.; Stephens, G. L.; Ringerud, M. A.; Coobs, C. L. *Bull. Am. Meteorol. Soc.* **1996**, *77*, 1233.
(60) Tiedje, H. F.; DeMille, S.; MacArthur, L.; Brooks, R. L. *Can. J. Phys.* **2001**, *79*, 773.
(61) Ma, Q.; Tipping, R. H. *J. Chem. Phys.* **2002**, *116*, 4102.
(62) Dyke, T. R.; Muenter, J. S. *J. Chem. Phys.* **1973**, *59*, 3125.
(63) Dyke, T. R.; Mack, K. M.; Muenter, J. S. *J. Chem. Phys.* **1977**, *66*, 498.